ELSEVIER

Available online at www.sciencedirect.com

ScienceDirect

Polymer 47 (2006) 6598–6605

polymer

www.elsevier.com/locate/polymer

Polybinaphthyls incorporating chiral 2,2′-binaphthyl and isoquinoline moieties by Sonogashira reaction

Yixiang Cheng*, Jinfeng Song, Xiaowei Zou, Shuwei Zhang, Yan Liu, Hui Huang

School of Chemistry and Chemical Engineering, Nanjing University, Nanjing, Jiangsu 210093, PR China

Received 13 April 2006; received in revised form 9 June 2006; accepted 15 July 2006

Abstract

Polymers **P-1**, **P-2**, **P-3**, **P-4** and **P-5** were synthesized by the polymerization of 5,8-bis(ethynyl)isoquinoline (**M-1**) with (*R*)-3,3′-diiodo-2,2′-bisbutoxy-1,1′-binaphthyl ((*R*)-**M-2**), (*S*)-3,3′-diiodo-2,2′-bisbutoxy-1,1′-binaphthyl ((*S*)-**M-2**), (*R*)-6,6′-dibromo-2,2′-bisbutoxy-1,1′-binaphthyl ((*R*)-**M-3**), (*S*)-6,6′-dibromo-2,2′-bisbutoxy-1,1′-binaphthyl ((*S*)-**M-3**), and *rac*-6,6′-dibromo-2,2′-bisbutoxy-1,1′-binaphthyl (**M-4**) under Sonogashira reaction, respectively. Both monomers and polymers were analyzed by NMR, MS, FT-IR, UV–vis spectroscopy, DSC–TGA, fluorescence spectroscopy, GPC and circular dichroism (CD) spectroscopy. CD spectra of polymers **P-1** and **P-2**, **P-3** and **P-4** are almost identical except that they gave opposite signals at each wavelength. The long wavelength CD effect of **P-1** and **P-2** can be regarded as the more extended conjugated structure in the repeating unit and the helical backbone in the polymer chain. All five polymers have strong blue-green fluorescence due to the efficient energy migration from the extended π-electronic structure of the repeating unit of the polymers to the chiral binaphthyl core and are expected to provide understanding of structure–property relationships of the chiral conjugated polymers.

Keywords: (*R*)- and (*S*)-BINOL; Chiral conjugated polymer; Isoquinoline

1. Introduction

Organic conjugated polymers based on π-conjugated organic molecules and chain backbone structures have attracted much interest during the past decade [1–3]. This kind of polymer materials with tunable optical and electronic properties can be achieved by the careful combination of the designed monomers. They can be used to prepare organic light-emitting diodes, electroluminescent devices, nonlinear optical materials, supramolecular sensors and full-color flat panel displays [4–7]. Chiral conjugated polymers are optically active materials made of organic fragments such as aromatic rings and unsaturated carbon or heteroatom bonds with delocalizable π-electronic system. Chiral BINOL and its derivatives are one of the most important C_2 symmetric compounds in the asymmetric synthesis field [8–10] and fluorescence sensors in chiral molecular recognition [11–13]. Recently, we have initiated a project to focus on the conjugated polybinaphthyls with a main chain chiral configuration. The chiral conjugated polybinaphthyls can lead to the properties of electro-optical sensors, asymmetric catalysis, enantioselective and molecular recognition by controlling the chiral organic groups and the linker structures at the well-defined molecular level [14–16].

In this paper, we chose an electron-deficient heterocyclic unit 5,8-bis(ethynyl)isoquinoline as the conjugated molecular bridge linker into the chiral polybinaphthyls' main chain backbone. Quinoline, isoquinoline, quinoxaline and oxadiazole derivatives have been widely used as electron transporting/hole blocking materials in LED devices and LED blends because this kind of unit has many excellent properties, such as better chromophore, high electron affinity, high thermal and oxidative stability, and good charge injection and transporting building blocks [3,5,6,15,17–22]. 5,8-Bis(ethynyl)isoquinoline is introduced into the polymer main chain to maintain conjugation

---

* Corresponding author. Tel.: +86 25 83592709; fax: +86 25 83317761.
E-mail address: yxcheng@nju.edu.cn (Y. Cheng).

0032-3861/$ - see front matter © 2006 Elsevier Ltd. All rights reserved.
doi:10.1016/j.polymer.2006.07.024

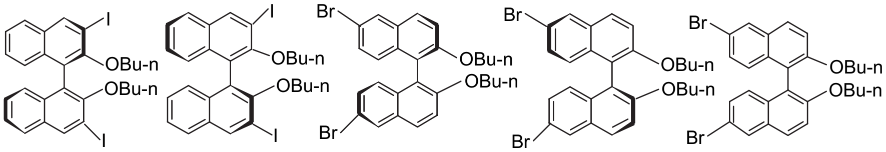

(*R*)-M-2 **(*S*)-M-2** **(*R*)-M-3** **(*S*)-M-3** **M-4**

Scheme 1. Molecular structure of chiral monomers and **M-4**.

between the isoquinoline and naphthyl segments so that the electron transporting properties of the polymers can be improved. In addition, by introducing the electron withdrawing isoquinoline moiety into the main chain, the electron density may shift away from the ethynyl bond, which could increase the stability of the resulting chiral polymers. (*R*)-**M-2**, (*S*)-**M-2**, (*R*)-**M-3** and (*S*)-**M-3** are chosen as the chiral monomers for the synthesis of the desired chiral polybinaphthyls. Attachment of the butoxy substituents on binaphthyl rings as the side chain of the polymers can not only modify the electronic properties and conjugated structure of these chiral polymers, but also improve the solubility dramatically in common organic solvents.

Sonogashira coupling reaction is one of the most important C–C coupling reactions in organic chemistry synthesis [23–29]. Herein, we report preliminary results of the synthesis of two kinds of polymers based on 3,3′- and 6,6′-positions of the 1,1′-binaphthyl unit by Pd-catalyzed Sonogashira cross-coupling reaction. All five polymers containing ethynyl linkage between naphthyl and isoquinoline group can reduce steric hindrance between backbone rings and groups, and also have a beneficial effect on delocalizable π-electronic conjugation structure of polymers. These polymers are expected to have potential application in blue-green light-emitting materials with significant fluorescence quantum efficiencies.

2. Experimental section

2.1. General

^{1}H, ^{13}C NMR spectra measurements (all in $CDCl_3$) were recorded on a 300-Bruker spectrometer with TMS as an internal standard. FT-IR spectra were recorded on a Nexus 870 FT-IR spectrometer. UV–vis spectra were obtained from a Perkin–Elmer Lambda 25 spectrometer. DSC–TGA was preformed on a Perkin–Elmer Pyris-1 instrument under N_2 atmosphere. Fluorescent spectra were obtained from a 48000 DSCF spectrometer. MS was determined on Micromass GCT. Circular dichroism was determined with a Jasco J-810 spectropolarimeter. Molecular weight was determined by gel permeation chromatography (GPC) with Waters-244 HPLC pump and THF was used as solvent and relative to polystyrene standards. All solvents and reagents were commercially available A.R. grade. (*R*)- and (*S*)-1,1′-binaphthol (BINOL) were purchased from Aldrich and directly used without purification. All reactions were performed under N_2 using Schlenk tube techniques. THF, *n*-butylamine and toluene were purified by distillation from sodium in the presence of benzophenone. CH_2Cl_2 and CH_3CN were distilled from P_2O_5.

2.2. Monomer syntheses

Molecular structures of chiral monomers and **M-4** are shown in Scheme 1. (*R*)-3,3′-Diiodo-2,2′-bisbutoxy-1,1′-binaphthyl ((*R*)-**M-2**) and (*S*)-3,3′-diiodo-2,2′-bisbutoxy-1,1′-binaphthyl ((*S*)-**M-2**) were synthesized according to literature [15]. (*R*)-6,6′-Dibromo-2,2′-bisbutoxy-1,1′-binaphthyl ((*R*)-**M-3**), (*S*)-6,6′-dibromo-2,2′-bisbutoxy-1,1′-binaphthyl ((*S*)-**M-3**) and (*rac*)-6,6′-dibromo-2,2′-bisbutoxy-1,1′-binaphthyl (**M-4**) were synthesized according to literature [14].

2.3. Preparation of 5,8-bis(ethynyl)isoquinoline (*M-1*)

5,8-Dibromoisoquinoline was synthesized according to literature [30] (Scheme 2). The crude product was recrystallized from methanol. Yield was 85%. Mp: 121–122 °C; MS *m/z*: 287 (M^+, 100), 206 (22), 127 (53); ^{1}H NMR: δ 7.79 (d, $J = 8.0$ Hz, 1H), 7.90 (d, $J = 8.0$ Hz, 1H), 8.10 (d, $J = 5.7$ Hz, 1H), 8.75 (d, $J = 6.0$ Hz, 1H), 9.66 (s, 1H); ^{13}C NMR: δ 119.2, 121.2, 122.2, 127.5, 131.5, 134.1, 136.3, 145.3, 152.3; $\nu_{\max}$ (KBr)/cm^{-1}: 1604.1, 1364.6, 1256.0, 971.8, 833.78, 818.8, 629.0.

5,8-Dibromoisoquinoline (2.31 g, 8.00 mmol), $Pd(OAc)_2$ (36 mg, 0.16 mmol), PPh_3 (168 mg, 0.64 mmol) and CuI (153 mg, 0.80 mmol) were mixed and dissolved in 80 mL Et_3N–THF (1:3 v/v) under N_2 atmosphere. Trimethylsilylethyne (2.67 mL, 24.00 mmol (delete)) was added to the above solution at room temperature. The reaction mixture was kept stirred at 35 °C for 8 h, and then the mixture was cooled to room temperature. The mixture was filtered through a short column of silica gel with ethyl acetate as eluent. After removal of the solvent, the crude 5,8-bis(trimethysilyethynyl)-isoquinoline was dissolved in Et_2O–MeOH (80 mL, 4:1 v/v). The solution was bubbled with N_2 for 10 min, and aqueous KOH (0.985 g, 17.6 mmol in 1 mL water) was added to the above solution. The mixture was stirred for 2 h at room temperature and then the solvent was removed under reduced pressure. The residue was extracted with CH_2Cl_2 (2 × 100 mL) and washed with saturated brine twice. The combined organic layers were dried over anhydrous $MgSO_4$. After the solvent was removed under reduced pressure, the crude product was purified on silica column by using the mixed solvents, petroleum ether and ethyl acetate (10:1 v/v), as the eluent to afford a pale yellow solid. Yield was 82% (1.42 g). **M-1** is stable in the air, but turned brown in the air at room temperature, it could be

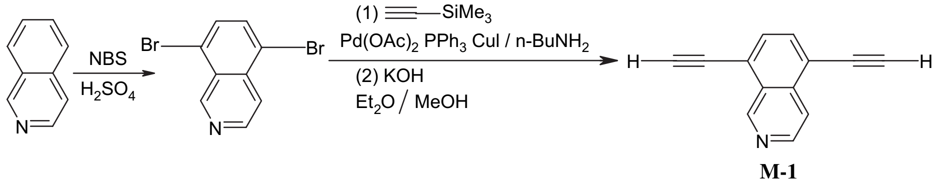

Scheme 2. Synthetic procedures of **M-1**.

preserved in CH_2Cl_2 at −4 °C before use. MS *m/z*: 177 (M^+, 100), 150 (36); ^{1}H NMR: δ 3.64 (1H, s), 3.68 (1H, s), 7.78 (d, $J = 7.5$ Hz, 1H), 7.89 (d, $J = 7.5$ Hz, 1H), 8.17 (dd, $J = 5.9$, 0.8 Hz, 1H), 8.70 (d, $J = 5.9$ Hz, 1H), 9.77 (d, $J = 0.8$ Hz, 1H); ^{13}C NMR: δ 79.9, 80.2, 85.3, 85.8, 119.1, 120.5, 121.7, 128.2, 132.0, 134.6, 136.6, 144.9, 151.5; ν_{max} (KBr)/cm^{-1}: 3237.3, 3201.5, 3069.1, 3026.3, 2097.5, 1696.5, 1686.3, 1603.0, 1558.8, 1373.5, 1296.0, 1282.4, 1234.6, 1212.6, 1176.7, 1035.4, 844.2, 828.9, 805.3, 747.6, 693.0, 650.0, 623.5.

2.4. Preparation of polymers

2.4.1. Preparation of **P-1**

A mixture of **M-1** (200.1 mg, 1.131 mmol) and (*R*)-**M-2** (734.9 mg, 1.131 mmol) was dissolved in 10 mL mixed solvents of 8 mL toluene and 2 mL *n*-$BuNH_2$. The solution was first bubbled with N_2 for 15 min before 4 mol% $Pd(PPh_3)_4$ (52 mg, 0.045 mmol) and 20 mol% CuI (44 mg, 0.23 mmol) were added to the above solution. The temperature of the mixture was kept at 80 °C for 3 d under N_2, and then was cooled to room temperature. After removal of the solvent, the residual solid was dissolved in 10 mL THF. The mixture was filtered through a short silica gel column into methanol (150 mL). Crude polymer **P-1** was precipitated in methanol, and then filtered and washed with methanol several times. Further purification could be conducted by dissolving the polymer in THF to precipitate in methanol again. **P-1** was dried in vacuum to give 675.6 mg in 85% yield (Scheme 3). **P-1** spectroscopic data: ^{1}H NMR: δ 0.50–0.52 (m, 6H), 0.82–0.95 (m, 4H), 1.27–1.38 (m, 4H), 3.82 (br, 2H), 4.17 (br, 2H), 7.21–7.33 (m, 6H), 7.37–7.49 (m, 2H), 7.81–7.98 (m, 4H), 8.36–8.43 (m, 2H), 8.73 (br, 1H); ν_{max} (KBr)/cm^{-1}: 3053.4, 2955.8, 2929.5, 2869.2, 2201.2, 1601.2, 1555.4, 1489.0, 1438.6, 1379.7, 1351.8, 1259.6, 1229.1, 1097.1, 1018.6, 888.9, 842.7, 748.9.

P-2, **P-3**, **P-4** and **P-5** were synthesized by using the same method as **P-1**.

P-2 spectroscopic data: ^{1}H NMR: δ 0.48–0.52 (m, 6H), 0.82–0.95 (m, 4H), 1.27–1.39 (m, 4H), 3.84 (br, 2H), 4.20 (br, 2H), 7.18–7.32 (m, 6H), 7.35–7.48 (m, 2H), 7.80–7.97 (m, 4H), 8.37–8.41 (m, 2H), 8.75 (br, 1H); ν_{max} (KBr)/cm^{-1}: 3053.5, 2955.5, 2930.1, 2869.3, 2201.4, 1601.3, 1554.7, 1489.6, 1439.8, 1379.9, 1351.7, 1228.4, 1062.7, 1017.8, 888.9, 842.4, 748.9.

P-3 spectroscopic data: ^{1}H NMR: δ 0.70 (br, 6H), 1.02 (br, 4H), 1.43 (br, 4H), 4.00 (br, 4H), 7.06–7.22 (m, 6H), 7.44 (br, 3H), 7.87 (br, 2H), 8.02 (br, 2H), 8.24 (br, 2H); ν_{max} (KBr)/cm^{-1}: 3043.6, 2955.4, 2929.6, 2869.2, 2197.4, 1587.7, 1490.5, 1464.9, 1377.9, 1341.3, 1271.0, 1243.7, 1068.5, 1030.5, 825.7.

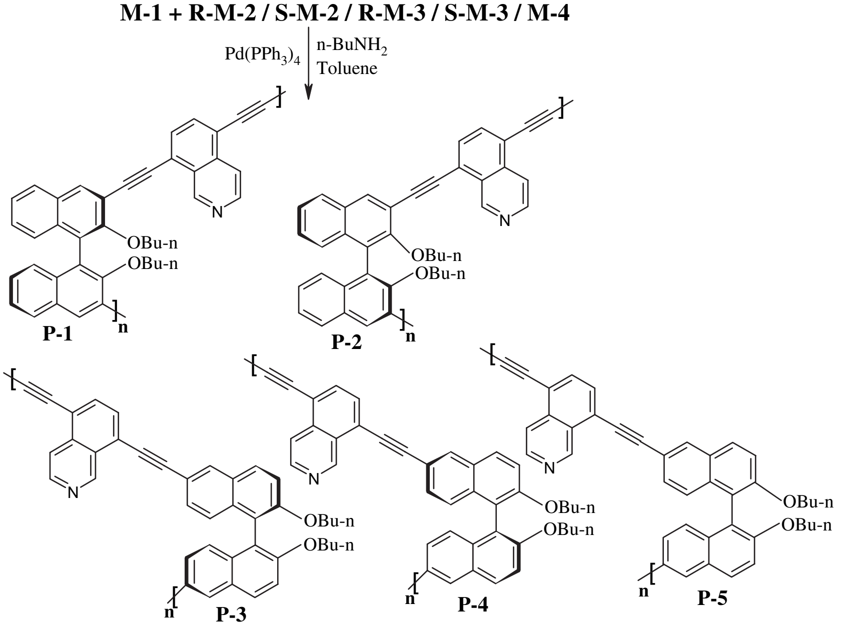

Scheme 3. Synthetic procedures of **P-1**, **P-2**, **P-3**, **P-4** and **P-5**.

P-4 spectroscopic data: ^{1}H NMR: δ 0.69 (br, 6H), 1.01 (br, 4H), 1.43 (br, 4H), 3.98 (br, 4H), 7.06–7.21 (m, 6H), 7.35–7.55 (m, 3H), 7.78–7.90 (m, 2H), 8.02 (br, 2H), 8.24 (br, 2H); ν_{max} (KBr)/cm^{-1}: 3044.9, 2955.9, 2929.2, 2869.0, 2195.8, 1587.0, 1491.0, 1465.2, 1377.2, 1341.7, 1261.5, 1091.1, 1069.0, 1029.1, 801.6.

P-5 spectroscopic data: ^{1}H NMR: δ 0.69 (br, 6H), 0.89–1.05 (m, 4H), 1.44 (br, 4H), 4.00 (br, 4H), 7.03–7.20 (m, 6H), 7.44 (br, 3H), 7.86 (br, 2H), 8.04 (br, 2H), 8.24 (m, 2H); ν_{max} (KBr)/cm^{-1}: 3044.0, 2956.2, 2929.5, 2869.4, 2197.8, 1588.0, 1490.8, 1465.9, 1378.7, 1341.6, 1268.7, 1091.2, 1069.0, 1029.7, 801.6.

3. Results and discussion

3.1. Syntheses and features of polymers

A general Sonogashira reaction condition was applied to the polymerization. In this paper, Pd(PPh$_3$)$_4$ was chosen as catalyst instead of PdCl$_2$(PPh$_3$)$_2$ [27,29,31]. The C–C cross-coupling process was easily carried out by the polymerization of **M-1** with (*R*)-**M-2**, (*S*)-**M-2**, (*R*)-**M-3**, (*S*)-**M-3** and **M-4** in the presence of a catalytic amount of Pd(PPh$_3$)$_4$ (4 mol%) and CuI (20 mol%) at 80 °C under the protection of N$_2$ atmosphere. Minor-groove polymers **P-1** and **P-2** were obtained at the 3,3′-positions of (*R*)-**M-2** and (*S*)-**M-2**, and major-groove polymers **P-3**, **P-4** and **P-5** were obtained at the 6,6′-positions of (*R*)-**M-3**, (*S*)-**M-3** and **M-4** [9,32]. The results of polymers' GPC determination show moderate molecular weight. GPC analysis and the specific rotation results of five polymers are listed in Table 1. Normally the reactivity order of organic halides for Sonogashira coupling reaction is vinyl iodide ~ vinyl triflate > vinyl bromide > vinyl chloride > aryl iodide > aryl bromide ≫ aryl chloride [27,28]. **P-1** and **P-2** have higher molecular weight and yields than **P-3**, **P-4** and **P-5** because (*R*)-**M-2** and (*S*)-**M-2** have higher activity for polymerization.

The chirality of 1,1′-binaphthol (BINOL) and its derivatives is derived from the restricted rotation of the two naphthalene rings. The rigid structure and C$_2$ symmetry of the chiral binaphthyl molecules can play important role in inherent chiral induction. The dihedral angle between two naphthalene rings of a binaphthyl molecule ranges from 60 to 120°, which leads to the kinked or twisted polymer main chain backbone [9,33–35]. According to Samyn's report [33,36], the chiral polymer incorporating chiral *R* or *S* binaphthyl units into the main chain of polymer backbone can adopt a helical configuration. But no helical configuration can be formed if racemic 1,1′-binaphthyl monomers are incorporated into the same polymer backbone, it may form a random-coil-like structure. He pointed out that polymers are helices due to the twisted configuration of the binaphthyl moieties if chiral binaphthyl units are connected through rigid groups. A helix is a highly regular structure in which all bonds that form the helix have the same configuration (either *R* or *S*). Kondo et al. also reported that the main chains composed of rigid segments are twisted to one-direction by the chiral binaphthyl linker and an ordered structure of the main chain backbone incorporating optically pure binaphthyls can adopt the stable helical configuration [37]. Yashima et al. thought the generation of a helical structure should result in significant chiral amplification [38]. In this paper, the absolute values of the special rotation ($[\alpha]_D^{25}$) of polymers **P-1** and **P-2** are much larger than **P-3** and **P-4**. As a result, four chiral polymers **P-1** and **P-2**, **P-3** and **P-4** are made of optically pure binaphthyl units. The optical rotations of **P-3** and **P-4** are a little larger than that of their chiral center units (*R*)- and (*S*)-2,2′-bisbutoxy-1,1′-binaphthyl, and CD spectra of **P-3** and **P-4** are very close to their corresponding monomers. According to Zhang and Pu's paper, [11] if polymers do not have a propagating helical chain conformation in solution, the optical rotation and CD spectrum of this polymer are very close to those of its monomeric model compound. That is, each unit in the polymer acts independently without an organized helical chain structure even though the 1,1-binaphthyl unit itself is helical. **P-3** and **P-4** may form zigzag chain configuration [11,39]. The special rotations and CD spectra signals of **P-1** and **P-2** are quite different from their corresponding monomers. Their specific rotations greatly increase and fluctuate to −788 and +822 ($c = 0.05$, THF). Dramatic changes are also observed in the CD spectra of the chiral polymers. A helical configuration of **P-1** and **P-2** should be generated according to their high special rotation values and strong CD spectra signals in the long wavelength centered at about 412 nm, which is attributed to the exciton coupling of the helical aromatic units [11].

Table 1
Polymerization results and characterization of **P-1**, **P-2**, **P-3**, **P-4** and **P-5**

	Yield (%)	M_w ($\times 10^3$)[a]	M_n ($\times 10^3$)[a]	PDI	$[\alpha]_D$[b]	T_g (°C)[c]	T_d (°C)[d]
P-1	85	9.7	4.2	2.30	−788	163	290
P-2	85	11.2	4.9	2.31	+822	171	293
P-3	65	7.2	3.2	2.25	−165	146	304
P-4	65	7.7	3.4	2.18	+148	152	290
P-5	65	6.1	2.1	2.88	0	141	293

[a] M_w, M_n and PDI of **P-1**, **P-2**, **P-3**, **P-4** and **P-5** were determined by gel permeation chromatography using polystyrene standards in THF.

[b] Temperature at 25 °C and solvent is THF ($c = 0.05$).

[c] Determined by DSC at a heating rate of 10 °C/min under N$_2$.

[d] Determined by TGA under N$_2$ at onset decomposition temperature.

3.2. Thermal analysis of polymers

All five polymers are air stable solid with brown color and show good solubility in THF, CH$_2$Cl$_2$, CHCl$_3$ and DMF. The nonplanarity of the polymers in the main chain backbone and flexible alkyl groups in the side chain can render the chiral polymers soluble in common organic solvents. Thermogravimetric analyses (TGA) of all polymers were carried out under N$_2$ atmosphere at a heating rate of 10 °C/min. The TGA plot of **P-1** is similar to that of **P-2**, and **P-3**, **P-4** and **P-5** are similar. **P-1**, **P-2**, **P-3**, **P-4** and **P-5** show the glass transition temperature (T_g) at 163, 171, 146, 152, 141 °C, respectively. The 3,3′-position polymers **P-1** and **P-2** have higher glass transition temperatures than the 6,6′-position polymers **P-3**, **P-4** and **P-5**. Racemic polymer **P-5** shows the lowest T_g.

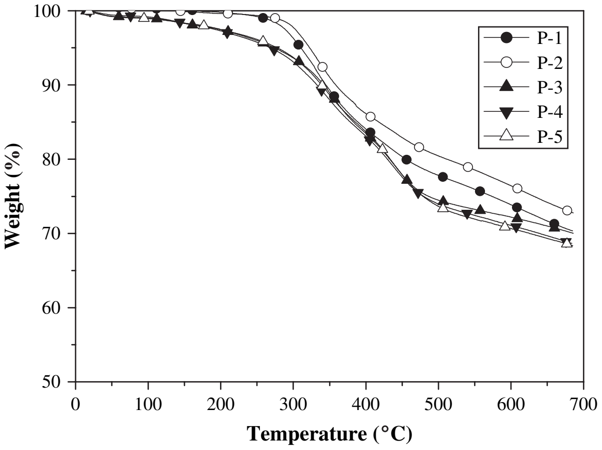

Fig. 1. TGA curves of **P-1**, **P-2**, **P-3**, **P-4** and **P-5**.

According to Fig. 1, there is no loss of weight before 300 °C for **P-1** and **P-2**, but there is about 5% loss of weight before 300 °C for **P-3**, **P-4** and **P-5**. **P-3**, **P-4** and **P-5** exhibit slow degradation rate. It can be ascribed to the reason that the stability of the butoxy group of the major-groove polymers **P-3**, **P-4** and **P-5** is lower than that of minor-groove polymers **P-1** and **P-2**, and can also be regarded that the helical configuration polymers **P-1** and **P-2** have higher stability than the zigzag configuration polymers **P-3** and **P-4**. Under N_2 atmosphere, an apparently one-step degradation is observed at temperature ranging from 300 to 650 °C. They tend to complete decomposition at 680 °C. A total loss of about 30% is observed when heated to 700 °C.

3.3. Optical properties

Figs. 2 and 3 illustrate the UV–vis absorption spectra and fluorescent spectra of polymers in THF solution and polymers as cast-spin films. Optical properties of all polymers are summarized in Table 2. UV–vis spectra of polymers **P-1** and **P-2** are similar, and UV–vis spectra of polymers **P-3**, **P-4** and **P-5** are similar due to the same polymer molecular chain structure. Compared to the repeating unit 2,2′-bisbutoxy-1,1′-binaphthyl and **M-1**, the polymers' UV absorption spectra display great red-shifts. The strongest UV absorption peaks λ_{max} of 2,2′-bisbutoxy-1,1′-binaphthyl and **M-1** appear at 235 and 346 nm, respectively. The strongest absorption wavelengths λ_{max} of **P-1** and **P-2** in THF solution appear at 386 nm. **P-1** and **P-2** show the stronger and broader absorption at the region from 340 to 450 nm than that of their corresponding monomers. The strongest absorption wavelengths λ_{max} of **P-3**, **P-4** and **P-5** in THF solution appear at 377 nm. **P-3**, **P-4** and **P-5** show the stronger and broader absorption at the region from 330 to 430 nm. The UV absorptions of thin films of 3,3′-position and 6,6′-position polymers show red-shifts of about 12 and 8 nm relative to those measured in solution state, respectively (Table 2). Pu synthesized a series of chiral conjugated polymers incorporating polybinaphthyls into the main chain and compared their UV absorption wavelengths of the polymers with their corresponding repeating units, and found that there is almost no extended conjugation across the 1,1′-bond of the binaphthyl units in the backbone of polybinaphthyl [9,40,41]. In this paper, a large red-shift in the electronic absorptions of the conjugated polymers can be attributed to the effective π–π* conjugated segment of the linker conjugated unit **M-1** and naphthyl group in the repeating unit of polybinaphthyls' main chain [14,15,42,43].

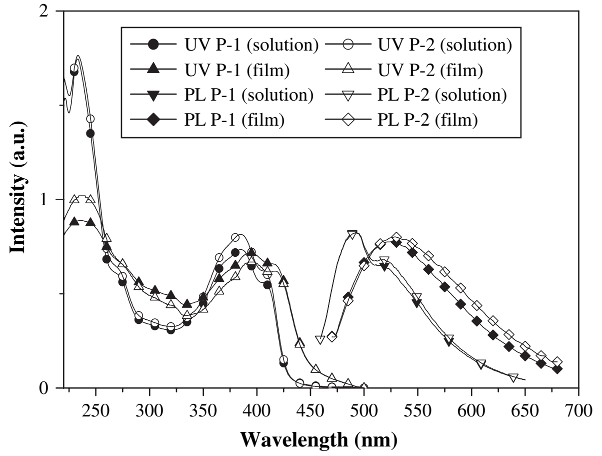

Fig. 2. UV–vis and fluorescence spectra of **P-1** and **P-2** in THF solution and cast-spin film.

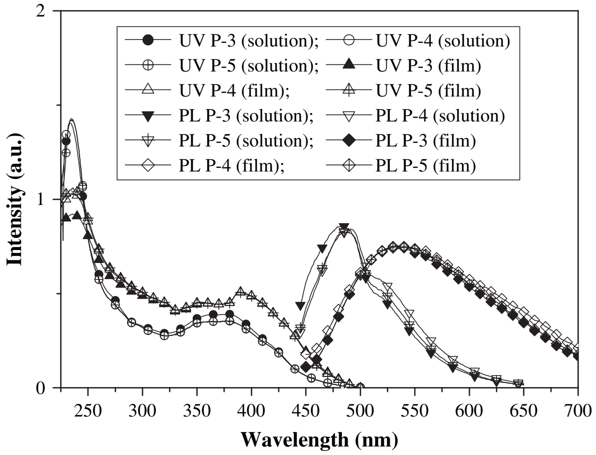

Fig. 3. UV–vis and fluorescence spectra of **P-3**, **P-4** and **P-5** in THF solution and cast-spin film.

Fluorescent spectra of all five polymers were determined in THF solution and in cast-spin films (Fig. 2). The fluorescent spectra of 3,3′-position and 6,6′-position polymers are similar due to the same chain structure except chiral center units. The polymers can emit blue-green light under UV (361 nm) or sunlight even in low concentration (1×10^{-4} mol/L). 2,2′-Bisbutoxy-1,1′-binaphthyl and **M-1** do not show visible fluorescence. The maximum fluorescent wavelengths λ^{F}_{max} of five polymers in THF solution are about 490 nm. Polymers show blue-green fluorescence due to the efficient energy transfer or exciton migration from the extended π-electronic structure of the repeating unit of polymer to the chiral binaphthyl core [15,42,44]. But in the solid film which was fabricated by spin

Table 2
Optical properties of **P-1**, **P-2**, **P-3**, **P-4** and **P-5**

	UV–vis (λ_{max})		PL (λ_{max})				Φ_{PL}[d]
	Solution (nm)[b]	Film (nm)[c]	Solution (nm)[b]		Film (nm)[c]		Solution
			λ_{ex}	λ_{em}	λ_{ex}	λ_{em}	
BINOL-OBu[a]	234	–	357	380		–	–
M-1	346	–	354	367, 386		–	–
P-1	408, 386	420, 397	446	491	460	525	0.36
P-2	408, 387	419, 398	449	492	460	527	0.32
P-3	377	385	433	491	460	529	0.26
P-4	377	385	433	491	460	530	0.32
P-5	377	385	435	488	460	530	0.34

[a] BINOL-OBu stands for 2,2′-bisbutoxy-1,1′-binaphthyl.
[b] Determined in THF solution.
[c] Determined in cast-spin film.
[d] These values were estimated by using the quinine sulfate solution (ca. 1.0×10^{-5} M) in 0.12 M H_2SO_4 ($\Phi_f = 55\%$) as a standard.

coating on ITO glass at a rate of 3000 rpm/min, the fluorescent wavelengths λ_{max}^{F} of **P-1**, **P-2**, **P-3**, **P-4** and **P-5** show red-shift of 24, 25, 28, 29 and 32 nm relative to those measured in solution state. It can be attributed to a higher conjugated structural stacking of the repeating unit in the solid than in the solution [43,45–47].

3.4. CD spectra

The special rotation values and CD spectral data of chiral monomers (*R*)-**M-2**, (*S*)-**M-2**, (*R*)-**M-3** and (*S*)-**M-3** can be found in literature [14,15]. Although the special rotation values ($[\alpha]_{\mathrm{D}}^{25}$) of chiral monomers (*R*)-**M-2**, (*S*)-**M-2**, (*R*)-**M-3** and (*S*)-**M-3** are −71.8 ($c = 0.5$, THF), +71.5 ($c = 0.5$, THF), +18.8 ($c = 0.1$, THF), −19.5 ($c = 0.1$, THF) [14,15] and that of the chiral center units (*R*)- and (*S*)-2,2′-bisbutoxy-1,1′-binaphthyl are +57.8 and −57.2, but $[\alpha]_{\mathrm{D}}^{25}$ of their conjugated polymers **P-1**, **P-2**, **P-3** and **P-4** are −788, +822, −165 and +148, respectively. The absolute values of the special rotation ($[\alpha]_{\mathrm{D}}^{25}$) of the four polymers are larger than their corresponding monomers and the chiral center units (*R*)- or (*S*)-2,2′-bisbutoxy-1,1′-binaphthyl. CD spectral data of **P-1**, **P-2** and **P-3**, **P-4** in CH_2Cl_2, $CHCl_3$ and THF are listed in Tables 3 and 4, respectively. The molecular ellipticity of (*R*)-2,2′-bisbutoxy-1,1′-binaphthyl is: $[\theta]_{\lambda_{(max)}} = +6.65 \times 10^5$ (225.9 nm), -10.4×10^5 (238.2 nm), $+0.66 \times 10^5$ (283.7 nm), and the molecular ellipticity of (*S*)-2,2′-bisbutoxy-1,1′-binaphthyl is: $[\theta]_{\lambda_{(max)}} = -6.60 \times 10^5$ (225.5 nm), $+10.6 \times 10^5$ (238.6 nm), -0.67×10^5 (284.2 nm). CD spectra of **P-1**, **P-2**, **P-3** and **P-4** show little change in three solvents, which demonstrates that all the four conjugated chiral polymers still keep similar configuration in these solvents. **P-1** and **P-2**, **P-3** and **P-4** exhibit intense CD signals with negative and positive cotton effects in their CD spectra, and their position and intensity are almost identical (Figs. 4 and 5). In addition, we found difference from the CD spectra of 6,6′-position monomers and their corresponding polymers **P-3** and **P-4**. Monomers (*R*)-**M-3** and (*S*)-**M-3** have the reversed signs of the special rotation for their corresponding polymers, but their cotton effect of CD spectra is consistent and CD signal intensities of the monomers are stronger than the corresponding polymers. There are great differences between (*R*)-**M-2**, (*S*)-**M-2** and their corresponding polymers. CD spectra of (*R*)-**M-2** and (*S*)-**M-2** are simpler, their ^1B_b bands appear at 231 and 249 nm. On the contrary, CD spectra of **P-1** and **P-2** become very complex. The major differences are from the long wavelength CD effect and the split of ^1B_b in the polymers even though their molar ellipticities are nearly the same magnitude as that of monomers (*R*)-**M-2** and (*S*)-**M-2**. **P-1** and **P-2** have ^1L_a bands at 269 and 270 nm, respectively. (*R*)-**M-1** and (*S*)-**M-1** did not have ^1L_a electronic transition in their CD spectra [39,48,49]. The long wavelength CD effect of polymers **P-1** and **P-2** appears at 356 and 358 nm, which can be regarded as due to the extended conjugated structure in the repeating unit and a high rigidity of polymer backbone [15,35,50,51]. The strongest and longest wavelengths' CD effect of polymers **P-1** and **P-2** appear at 411 and 412 nm, which can be attributed to the helical configuration backbone of the

Table 3
CD spectral data of **P-1** and **P-2**

	P-1 × 10^5 (in CH_2Cl_2)	**P-2** × 10^5 (in CH_2Cl_2)	**P-1** × 10^5 (in $CHCl_3$)	**P-2** × 10^5 (in $CHCl_3$)	**P-1** × 10^5 (in THF)	**P-2** × 10^5 (in THF)
$[\theta]$ (λ_{max} in nm)	+0.98(223.1)	−0.55(221.2)			+0.94(223.1)	−0.84(222.5)
	−3.05(236.0)	+2.86(236.4)	−3.30(237.9)	+2.56(238.5)	−2.97(235.8)	+2.74(235.8)
	+1.05(252.6)	−1.10(250.3)	+0.67(258.6)	−0.97(253.9)	+0.95(251.7)	−0.92(255.0)
	+1.12(264.1)	−1.11(264.2)	+1.06(265.5)	−1.06(262.7)	+1.02(262.0)	−0.97(264.1)
	+0.76(355.5)	−0.99(357.6)	+0.68(353.1)	−0.96(355.4)	+0.63(353.4)	−0.50(350.1)
	−1.50(396.8)	+2.29(395.3)	−1.68(396.6)	+2.48(397.6)	−1.56(394.3)	+1.65(394.5)
	−2.09(411.3)	+3.15(412.1)	−2.06(415.2)	+3.15(413.9)	−2.09(412.4)	+1.80(411.9)

Table 4
CD spectral data of **P-3** and **P-4**

	P-3 × 10^5 (in CH_2Cl_2)	**P-4** × 10^5 (in CH_2Cl_2)	**P-3** × 10^5 (in $CHCl_3$)	**P-4** × 10^5 (in $CHCl_3$)	**P-3** × 10^5 (in THF)	**P-4** × 10^5 (in THF)
[θ] (λ_{max} in nm)	+2.13(233.4) −1.14(249.6)	−2.30(233.5) +1.53(246.8)	+2.25(234.7) −1.42(253.9)	−1.68(234.0) +0.94(249.6)	+2.14(233.3) −1.04(251.5)	−1.63(233.6) +1.19(247.2)

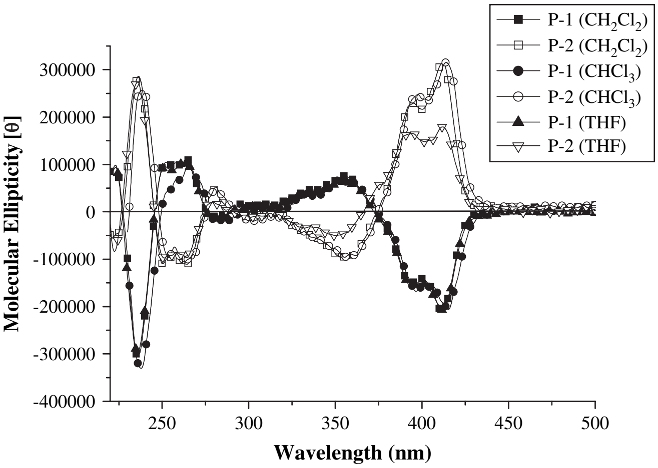

Fig. 4. CD spectra of **P-1** and **P-2**.

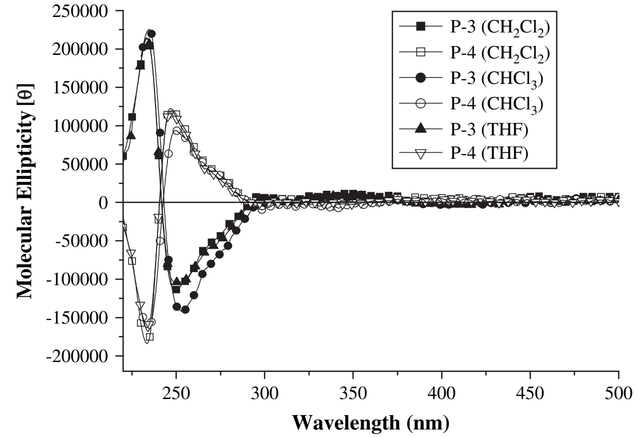

Fig. 5. CD spectra of **P-3** and **P-4**.

conjugated polymer chains. This is the main difference from zigzag polymer backbone of major-groove polymers **P-3** and **P-4** at 6,6′-position of binaphthyl.

4. Conclusions

Sonogashira reaction was found to offer a simple access to the chiral conjugated polymers. All five polymers show good solubility in some common solvents due to the nonplanarity of the twisted polymers in the main chain backbone and flexible alkyl substitutents on binaphthyl rings as side chain of the polymers. Polymers have strong blue-green fluorescence due to the efficient energy migration from the extended π-electronic structure of the repeating unit of the polymers to the chiral binaphthyl core and are expected to have potential application in the materials of fluorescent sensors. **P-1**, **P-2**, **P-3** and **P-4** exhibit strong CD signals with positive and negative cotton effect in their CD spectra. The major difference between 3,3′- and 6,6′-position polymers is that minor-groove polymers at 3,3′-position of binaphthyl adopt the helical configuration and major-groove position polymers at 6,6′-position of binaphthyl form zigzag backbone in the polymer main chain.

Acknowledgements

This work was supported by the National Natural Science Foundation of China (no. 20474028) and Jiangsu Provincial Natural Science Foundation (no. BK2004086).

References

[1] Yu WL, Meng H, Pei J, Huang W, Li YF, Heeger AJ. Macromolecules 1998;31:4838–44.
[2] Bredas JL, Deljonne D, Coropcean V, Cornil J. Chem Rev 2004;104:4971–5003.
[3] Kulkarni AP, Zhu Y, Jenekhe SA. Macromolecules 2005;38:1553–63.
[4] Hwang SW, Chen Y. Macromolecules 2002;35:5438–43.
[5] Zhan XW, Liu YQ, Wu X, Wang S, Zhu DB. Macromolecules 2002;35:2529–37.
[6] Peng ZH, Bao ZN, Galvin ME. Adv Mater 1998;10:680–3.
[7] Zhou G, Cheng YX, Wang LX, Jing XB, Wang FS. Macromolecules 2005;38:2148–53.
[8] Xu MH, Lin J, Hu QS, Pu L. J Am Chem Soc 2002;124:14239–46.
[9] Pu L. Chem Rev 1998;98:2405–94.
[10] Fan QH, Li YM, Chan ASC. Chem Rev 2002;102:3385–466.
[11] Zhang HC, Pu L. Macromolecules 2004;37:2695–702.
[12] Pu L. Chem Rev 2004;104:1687–716.
[13] Li ZB, Pu L. Org Lett 2004;6:1065–8.
[14] Cheng YX, Chen LW, Song JF, Zou XW, Liu TD. Polym J 2005;17:355–62.
[15] Cheng YX, Chen LW, Zou XW, Song JF, Wang ZL. Polymer 2006;47:435–40.
[16] Song JF, Cheng YX, Chen LW, Zhou XW, Wang ZL. Eur Polym J 2006;42:663–9.
[17] Kim JL, Kim JK, Cho HN, Kim DY, Hong SI. Synth Met 2000;114:97–100.
[18] Tonzola CJ, Alam MM, Jenekhe SA. Macromolecules 2005;38:9539–47.
[19] Tonzola CJ, Alam MM, Bean BA, Jenekhe SA. Macromolecules 2004;37:3554–63.
[20] Chen XLD, Jenekhe SA. Macromolecules 2001;34:3607–14.
[21] Jonforsen M, Johansson T, Inganas O, Andersson MR. Macromolecules 2002;35:1638–43.
[22] Bangcuyo CG, Rampey-Vaughn ME, Quan LT, Angel SM, Smith MD, Bunz UHF. Macromolecules 2002;35:1563–8.
[23] Sonogashira K, Tohda Y, Hagihara N. Tetrahedron Lett 1975;4467–70.
[24] Thorand S, Krause N. J Org Chem 1998;63:8551–3.
[25] Jones GB, Wright JM, Ploured GW, Hynd G, Huber RS, Mathews JE. J Am Chem Soc 2000;122:1937–44.
[26] Wang WL, Xu JW, Lai YH, Wang FK. Macromolecules 2004;37:3546–53.

[27] Sonogashira K. J Organomet Chem 2002;653:46–9.

[28] Alami M, Linstrumelle G. Tetrahedron Lett 1991;32:6109–12.

[29] Ma L, Hu QS, Musick KY, Vitharana D, Wu C, Kwan CMS, et al. Macromolecules 1996;29:5083–90.

[30] Brown WD, Gouliaev AH. Synthesis 2002;83–6.

[31] Khan MS, Al-Suti MK, Al-Mandhary MRA. Dalton Trans 2003;65–73.

[32] Hu QS, Huang WS, Vitharana D, Zheng XF, Pu L. J Am Chem Soc 1997; 119:12454–64.

[33] Koeckelberghs G, Vangheluwe M, Picard I, Groof L, Verbiest T, Persoons A, et al. Macromolecules 2004;37:8530–7.

[34] Ma L, Hu QS, Vitharana D, Wu C, Kwan CMS, Pu L. Macromolecules 1997;30:204–18.

[35] Chow HF, Ng MK. Tetrahedron Asymmetry 1996;7:2251–62.

[36] Koeckelberghs G, Verbiest T, Vangheluwe M, Groof L, Asselberghs I, Picard I, et al. Chem Mater 2005;17:118–21.

[37] Kondo F, Takahashi D, Kimura H, Takeishi M. Polym J 1998;30:161–2.

[38] Yashima E, Maeda K, Nishimura T. Chem Eur J 2004;10:43–51.

[39] Ma L, White PS, Lin WB. J Org Chem 2002;67:7577–86.

[40] Musick KY, Hu QS, Pu L. Macromolecules 1998;31:2933–42.

[41] Hu QS, Vitharana D, Liu G, Jain V, Pu L. Macromolecules 1996;29: 5075–82.

[42] Meng Y, Williams TS, Wang D, Liu TF, Chow HJ, Li C. Tetrahedron Asymmetry 1998;3693–707.

[43] Cha SK, Choi SH, Kim K, Jin JII. J Mater Chem 2003;13:1900–4.

[44] Jen AKY, Liu Y, Hu QS, Pu L. Appl Phys Lett 1999;75:3745–7.

[45] Lere-Porte JP, Moreau JJE, Serein-Spirau F, Torreilles C, Righi A, Sauvajol JL. J Mater Chem 2000;10:927–32.

[46] Bouachrine M, Lere-Porte JP, Moreau JJE, Serein-Spirau F, Torreilles CJ. Chem Mater 2000;10:263–8.

[47] Li H, Powell DR, Firman TK, West R. Macromolecules 1998;31: 1093–8.

[48] Mason SF, Seal RH. Tetrahedron 1974;30:1671–82.

[49] Kuroda R, Mason SF. Tetrahedron 1981;37:1995–9.

[50] Cheng H, Ma L, Hu QS, Zheng XF, Aderson J, Pu L. Tetrahedron Asymmetry 1996;7:3083–6.

[51] Cheng H, Pu L. Macromol Chem Phys 1999;200:1274–83.